Electromagnetic Analysis of a Flat-Type Proportional Solenoid by the Reluctance Method

Yeh-Sun Hong[1,#] and Yong-Cheol Kwon[2]

1 Faculty of Aerospace and Mechanical Engineering, Hankuk Aviation University Goyang, South Korea
2 Graduate School of Aerospace and Mechanical Engineering, Hankuk Aviation University, Goyang, South Korea
Corresponding Author / E-mail: yshong@hau.ac.kr, TEL: +82-2-300-0287, FAX: +82-2-3158-2988

KEYWORDS : Flat-type solenoid, Equivalent circuit, Reluctance model, Sensitivity analysis

In this study, the electromagnetic characteristic of a flat-type two-dimensional proportional solenoid were analyzed by the magnetic reluctance method. The magnetic equivalent circuit equation for the solenoid was derived by modeling the reluctance of air gaps and magnetic structural components such as pole core, armature and yoke. It was solved iteratively because of the nonlinear magnetization properties of iron parts. The solutions showed good agreement with experimental data. Based on the magnetic equivalent circuit equation, the influence of design parameters on force-to-armature displacement curves was mathematically derived and experimentally verified. In this way, dominant design parameters could be analytically determined.

Manuscript recieved: July 12, 2005 / Accepted: October 28, 2005

NOMENCLATURE

A = Cross-sectional area of magnetic flux path(m^2)
B = Magnetic flux density(Wb/m^2)
F = Magnetic force(N)
H = Magnetic field intensity(A-turns/m)
I = Electrical current(A)
L_i = Design parameter
μ = Permeability(H/m)
N = Winding number(turns)
l = Mean length of magnetic flux path(m)
mmf = Magnetomotive force(A·turn)
ϕ = Magnetic flux(Wb)
R = Reluctance(A-turns/Wb)
S_i = Sensitivity
T = Torque(Nm)
θ = Armature angle(deg)
W_m = Magnetization energy(J)

1. Introduction

Proportional solenoids for activating hydraulic or pneumatic valves in proportion to electrical signal have in general axisymmetric structure and their main feature is that the magnetic force induced by coil current does not change steeply in spite of plunger movement[1].

In case of small-sized pneumatic valves whose max. flow rate is less than 100 l/min, a proportional solenoid with max. force less than 5 N will be strong enough to operate them[2]. Therefore, miniaturized proportional solenoids are frequently required whose volume is appropriate for small-sized valves.

In general, the conventional axisymmetric proportional solenoids should install special guide bearings or membrane-type springs inside of their body to precisely support their armature. In this way, the sliding friction on the push rod extending through pole and that on the armature can be significantly reduced. However, miniaturizing whole solenoid structure is a difficult problem to solve because there is structural limit to reduce or save the required space for installing such additional components. This is the reason why a flat-type proportional solenoid basically suitable for miniaturization was invented[3].

The flat-type proportional solenoid has planar structure composed of armature rotating within limited angle range, pole with vertical and horizontal air gaps (air gap1 and air gap2, respectively), yoke and coil, as shown in Fig. 1. The force-to-armature displacement characteristics to be obtained here are that the force components induced in the vertical and horizontal air gaps should provide constant torque on the armature independent of its rotation angle, with respect to the hinge point. This requirement is essential for changing the armature angle in proportion to the input current, I by combining the solenoid with spring load. The push arm depicted in Fig. 1 is provided to push a valve element, where the force, F is proportional to the torque generated on the armature.

Since the two-dimensional flat-type proportional solenoid has a rotary armature making simple line contact with the pivot edge of yoke as hinge support, it has the advantage that the friction force on armature can be almost eliminated. And its structural components can be produced with high precision by such simple planar machining process as wire cutting. Besides, they are very easy to assemble.

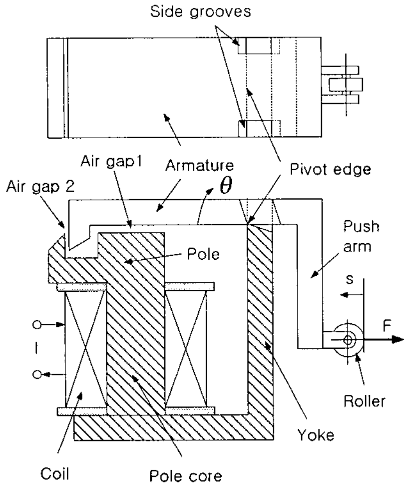

Fig. 1 Structure of a flat-type proportional solenoid

Hong[3] introduced the design process of the flat-type proportional solenoid using a commercial finite element analysis program, where it was based on a trial and error approach. And the flow control of a miniature double flapper nozzle valve using the flat-type proportional valve was realized and tested to show that the performance of the flat-type solenoid is almost equivalent to that of the conventional axisymmetric type.

Though focused on the conventional axisymmetric proportional solenoids, the study of Song[4] employed the reluctance method to examine the influence of its design parameters on the static performance. This study showed that the analysis results inevitably deviated more or less from the actual data because the reluctance method had the difficulty to precisely include the local magnetic saturation of magnetic structures in the equivalent circuit analysis model.

In general, the finite element method is widely applied to investigate the cause and effect of the design parameters for electromagnets because it allows precise modeling of them. However, the magnetic equivalent circuit analysis method is still advantageous to the finite element method when it is required to analytically figure out the relationships between design parameters and magnetic output force[5,6,7].

In this study, the flat-type proportional solenoid was modeled as a magnetic equivalent circuit, whose equation was solved to compute the static magnetic force-to-armature displacement characteristics. These were then compared with the experimental data to verify the accuracy of the reluctance model. Thereafter, the influence factors of each design parameter on the static characteristics of the proportional solenoid were analytically derived from the reluctance model. By quantitative comparison of them, the most sensitive design parameters were finally extracted. This whole process will be described in the following.

2. Derivation of a magnetic equivalent circuit for the flat-type proportional solenoid

When the operation of an electromagnet is analyzed by means of magnetic equivalent circuit, the reluctance of air gaps and magnetic structures are mathematically modeled to constitute a circuit equation. Then this circuit equation is solved for magnetic flux which is equivalent to the current in an electric circuit. Once the magnetic flux is obtained, the magnetic energy stored in electromagnet can be calculated. And the magnetic force induced in each air gap is determined by the rate of change of magnetic energy stored in the air gap with the armature displacement. Therefore, if any type of an electromagnet is expressed by a magnetic equivalent circuit, the influence of its design parameters such as shape and size of air gaps on magnetic force induction can be analytically examined.

According to Ampere's law, the magnetomotive force, *mmf* exciting an electromagnet by the electrical current, *I* applied to a coil with *N* turns, is expressed by:

$$mmf = NI = \int H\,dl = \int \frac{B}{\mu}\,dl \tag{1}$$

where the magnetic field intensity, H and the magnetic flux density, B are related by $B = \mu H$. μ denotes the permeability of magnetic structure and ℓ the mean length of magnetic flux path. Since the magnetic flux density, B is equal to the magnetic flux, Φ divided by the cross-sectional area A, Eq. (1) can be rewritten as:

$$mmf = NI = \int \frac{\phi}{\mu A}\,dl = \phi \int \frac{1}{\mu A}\,dl \tag{2}$$

As the reluctance, R is defined by the following expression[8]:

$$R = \int \frac{1}{\mu A}\,dl \tag{3}$$

Eq. (2) can be replaced by:

$$mmf = \phi R \tag{4}$$

If Eq. (4) is compared with the electric circuit expression for Ohm's law, *mmf* is analogous to voltage and Φ to current.

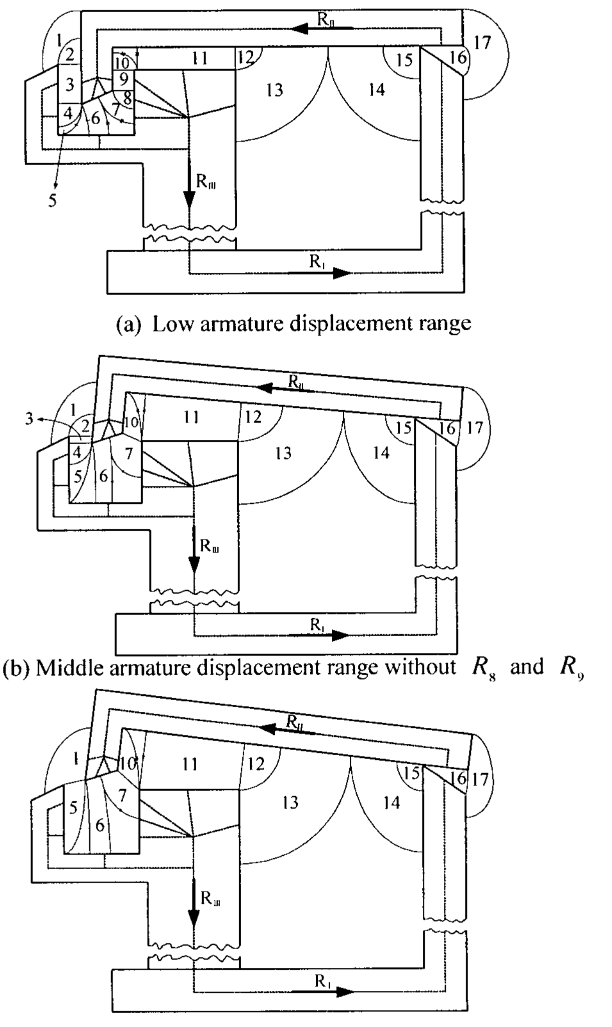

(a) Low armature displacement range

(b) Middle armature displacement range without R_8 and R_9

(C)High armature displacement range without R_2, R_3 and R_4

Fig. 2 Magnetic reluctance model

Generally speaking, the total reluctance of an electromagnet can be resolved into the reluctances of iron parts and those of air gaps encountered along the magnetic flux path. In this study, the flux path of the proportional solenoid was classified into three forms as shown in Fig. 2, according to the critical armature angles where the primary reluctances R_3 and R_9 in the horizontal air gap fade out in their turns while the armature angle increases. Finally, if the reluctances of each magnetic flux path are modeled by applying Eq. (3), the magnetic equivalent circuit for the proportional solenoid can be represented by Fig. 3.

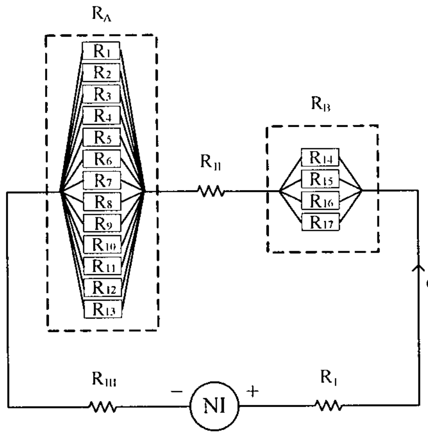

Fig. 3 Magnetic equivalent circuit

In this figure, R_I, R_{II} and R_{III} denote the reluctance of yoke, armature, and pole, respectively. The reluctances of each magnetic flux path between pole and armature are expressed by R_1 through R_{13}, while those between yoke and armature by R_{14} through R_{17}, with fringing effect considered.

As the magnetomotive force is analogous to the supply voltage and the magnetic flux to the current in an electric circuit, this equivalent circuit implies that the supply voltage is resolved into the voltage drops across the resistances of iron parts and air gaps. Therefore, the total reluctance of the magnetic equivalent circuit is given by:

$$R_{eq} = R_A + R_B + R_{steel} \tag{5}$$

where the total reluctance of yoke, armature and pole made of soft-magnetic material is equal to:

$$R_{steel} = R_{\mathrm{I}} + R_{\mathrm{II}} + R_{\mathrm{III}} = \sum_{i=1}^{\mathrm{III}} H_i l_i \tag{6}$$

The field intensities, H_I, H_{II} and H_{III} are in functional relationship with the magnetic flux densities in yoke, armature and pole, respectively, which is given by the magnetization curve of magnetic material. ℓ_I, ℓ_{II} and ℓ_{III} are the mean lengths of magnetic flux path for these three parts, respectively.

The reluctance of the air gap, R_A is equivalent to the sum of the parallel reluctances from R_1 to R_{13} and the reluctance, R_B to that from R_{14} to R_{17}. As already mentioned above, the reluctances of each magnetic flux path in the air gap can be derived by general application of Eq. (3). If R_{eq} is obtained, the magnetic flux encountered in the electromagnet can be calculated by:

$$\phi = \frac{NI}{R_{eq}} \tag{7}$$

The equivalent reluctance, R_{eq} is the function of magnetic flux density. The magnetization curve of magnetic materials which determine the relationship between the magnetic flux density and R_{eq}, is not linear, considering its saturation region. Therefore, Eq. (7) is implicit and can be only numerically solved for the magnetic flux by an iterative approach.

The ultimate goal of magnetic equivalent circuit analysis is to calculate the armature torque, T with respect to the pivot hinge as the armature angle, θ changes. While the magnetic energy stored in the solenoid is defined by the following expression:

$$W_m = \frac{\phi \cdot mmf}{2} = \frac{\phi^2 R_{eq}}{2} \tag{8}$$

the armature torque is equal to its rate of change with the armature rotation: i.e.

$$T = -\frac{dW_m}{d\theta} \tag{9}$$

3. Design parameters for flat-type proportional solenoid and computed results of its static characteristics

The equivalent reluctance, R_{eq} expressed by Eq. (5) is determined by the design parameters which are defined to be independent from each other as shown in Fig. 4. In this figure, the origin of the XY coordinate system attached on the armature is fixed on the pivoting point. And the thickness, L_z is constant for all the parts of flat-type proportional solenoid.

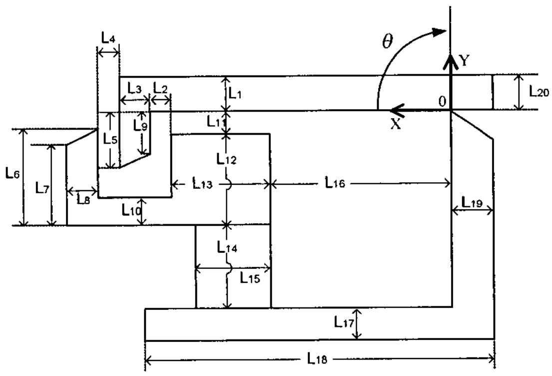

Fig. 4 Design parameters for flat-type proportional solenoid

Considering that the force produced on the roller tip of push arm, F is equivalent to the anticlockwise torque induced on the armature, T, the max. armature rotation range where F is kept constant, the max. value of F and the gradient of force-to-armature displacement curves can be treated as the important criterion representing the static characteristics of proportional solenoid. Among them, the armature rotation range and the max. force are significantly influenced by the armature length ($L_3+L_2+L_{13}+L_{16}$), the width (L_{11}) and length (L_{13}) of vertical air gap including its distance from pivot hinge (L_{16}), and the length (L_4) and the width (L_5, L_6) of horizontal air gap[3].

However, the gradient of force-to-displacement curves can not be estimated directly from the design parameters because it results from the complex process caused by the non-linear change of the reluctance of pole core, R_{III} and the saturation property of magnetic materials. But its desired value is to be iteratively followed after by a trial and error approach.

Table 1 Design parameters

Item	Value(mm)	Item	Value(mm)	Item	Value (mm)
L_1	2	L_8	2	L_{15}	2.5
L_2	0.525	L_9	1.6	L_{16}	11.5
L_3	2	L_{10}	2	L_{17}	2
L_4	0.5	L_{11}	0.35	L_{18}	21.5
L_5	2.55	L_{12}	4.55	L_{19}	2
L_6	4.55	L_{13}	7	L_{20}	1
L_7	3.55	L_{14}	16.45	L_Z	12

Table 1 shows the design parameters for the flat-type proportional solenoid which was provided as reference model for experimental verification of computed results from magnetic equivalent circuit analysis. The prototype of proportional solenoid shown in Fig. 5 was preliminarily designed by using a commercial finite element analysis program so that it basically exhibits the linear characteristics of proportional solenoids.

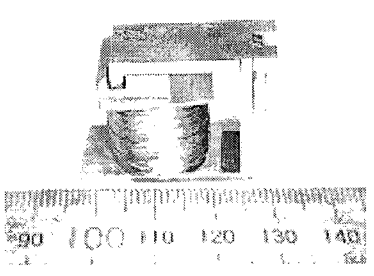

Fig. 5 Prototype of flat-type proportional solenoid

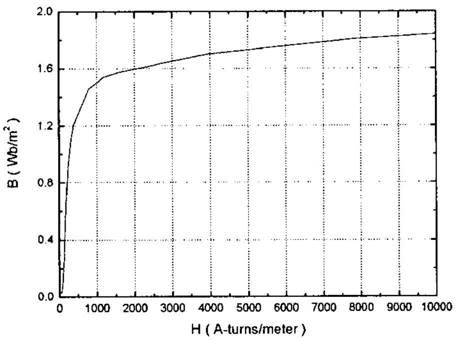

Fig. 6 Magnetization curve of iron parts

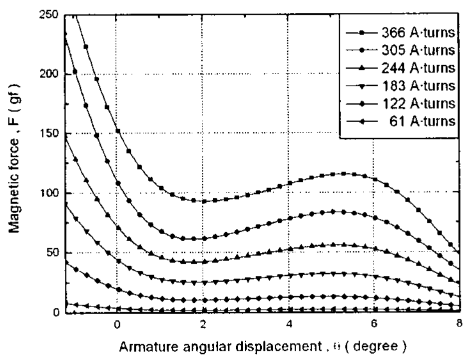

(a) Computed data

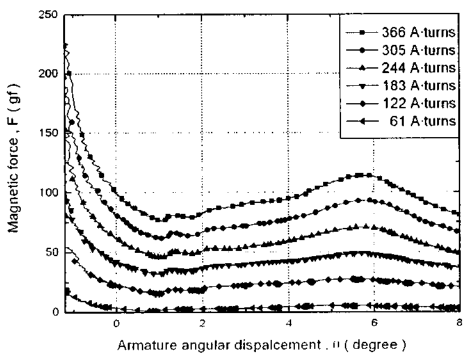

(b) Measured data

Fig. 7 Comparison of measured and computed force to-armature displacement curves

In order to make the prototype of proportional solenoid, a widely applied, low-carbon steel (S10C) was used. Fig. 6 depicts its magnetization curve which can be easily referred to material data books[8]. The accuracy of computed results does not absolutely rely on how precise the magnetization curve is represented, because the magnetic equivalent circuit model is an approximated mathematical expression. However, it was stressed in this study that the magnetization curve data should be as accurate as possible.

As shown in Fig. 7, the output force on the roller tip of push arm, F was computed and compared with the measured data, when the designed data in Table 1 was applied with NI changed to 61, 122, 183, 244, 305 and 366 A·turns, respectively. Here, the relationship between the magnetic force, F and the torque generated on armature, T was given by $F=T\div$ (vertical length of push arm).

If we compare the armature displacement range where the force is kept unchanged, the max. force and the gradient of force-to-displacement curves between two results, the computed data coincides with the measured very closely. In this study, the armature displacement range was divided into three regions by the boundary angles of 3.7° and 5.9° according to geometrical conditions, in order to model the reluctance of the air gap.

Fig. 8 illustrates the computed armature torque component induced in the vertical air gap comprising the reluctances R_{l1}, R_{l2} and R_{l3} and that induced in the other air gaps comprising from R_l to R_{l0}, where the pivoting hinge was considered as reference point.

The counterclockwise torque component induced in the vertical air gap, T_v decreased as the armature angle increased. But the torque component induced in the other air gaps, T_h increased until the armature angle reached 6° starting from 0° and decreased again thereafter. As a consequence, the total torque resulting from them remains almost constant within the armature displacement range between 1° and 6°. Therefore, it can be deduced that the design parameters expressing the "┌"- shaped armature end will determine the relationship between magnetic force and armature angle.

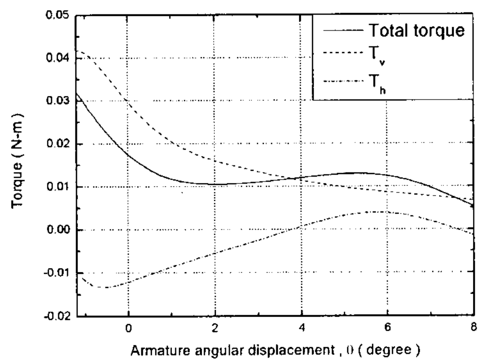

Fig. 8 Torque components induced in horizontal and vertical air gaps

4. Sensitivity analysis of design parameters

If the gradient of magnetic force- or torque-to-armature displacement curve is defined as k, it is equal to:

$$k = \frac{dT}{d\theta} = -\frac{d^2 W_m}{d\theta^2} \tag{10}$$

And if the intensity how strong this gradient is influenced by each design parameter, is defined as sensitivity S_i, it can be expressed by:

$$S_i = \frac{\partial k}{\partial L_i} = -\frac{\partial}{\partial L_i}\left(\frac{d^2 W}{d\theta^2}\right) \tag{11}$$

Fig. 9 depicts the sensitivities of the design parameters from L_l to L_{l3}, which were computed when the armature angle was θ =2°, 3° and 4°, respectively. According to the results, when θ =2°, the sensitivity of L_{11} has the largest positive value. That is, if the initial length of vertical air gap is made larger than the reference value in Table 1, it will make the magnetic force increase to the largest extent, as the armature angle changes positively in the vicinity of $\theta = 2°$. However, when $\theta = 4°$, the sensitivity of L_4 has the largest negative value. It means that the increase of the length of horizontal air gap from its reference value will make the magnetic force decrease to the largest extent with the positive change of armature angle in the vicinity of $\theta = 4°$.

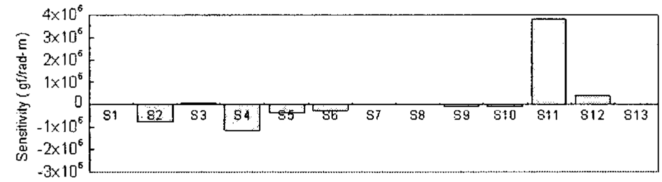

(a) $\theta = 2°$

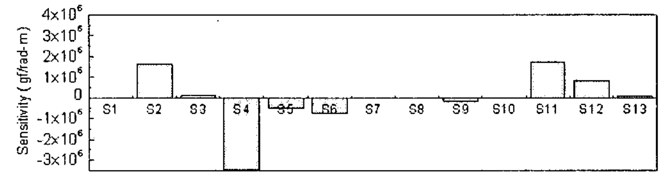

(b) $\theta = 3°$

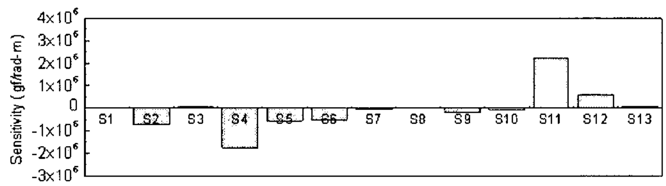

(c) $\theta = 4°$

Fig. 9 Sensitivity of design parameters

In order to verify the sensitivity analysis results, a new set of force-to-armature displacement curves were computed with L_4 increased, as shown in Fig. 10. It can be seen that within the armature angle range between 2° and 4°, the larger L_4 is, the more the gradient of force-to-armature displacement curve decreases.

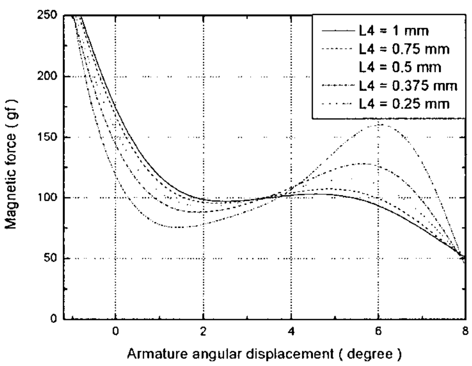

Fig. 10 Influence of L_4 on force-to-armature displacement curves

Fig. 11 shows experimental results that obtained when L_4 was increased from 0.5mm applied in Fig. 7, to 1mm. The gradient of force-to-armature displacement decreased and became almost horizontal.

As another computation example, Fig. 12 depicts that, if L_{11} was made larger, the gradient of force-to-armature displacement curve became larger within its displacement range between 2° and 4°. This tendency was most strong in the vicinity of 2° as already explained in Fig. 9. Considering the general features of on-off solenoids, it can be said without experimental examination that this results reflect the actual phenomena very well.

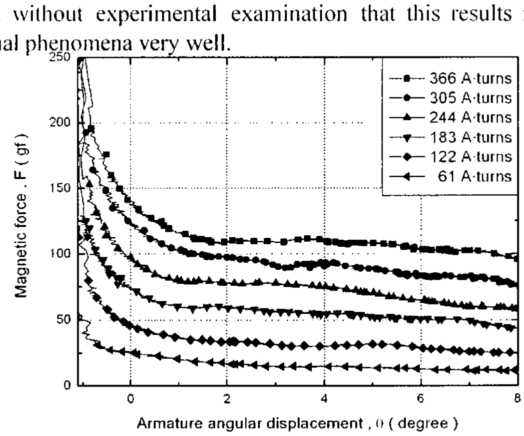

Fig. 11 Measured force-to-armature displacement curves with increased L_4

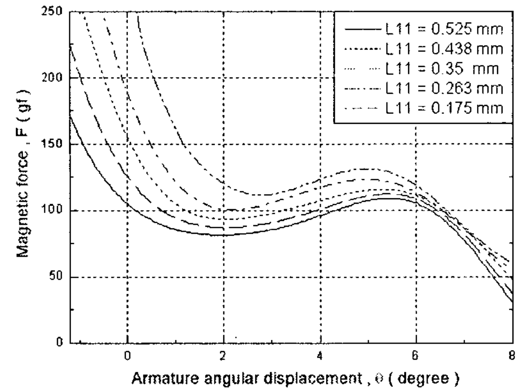

Fig. 12 Influence of L_{11} on force-to-armature displacement curves

In similar way, the sensitivity of magnetic force magnitude to design parameters were defined as follows and calculated as shown in Fig. 13:

$$S_i' = \frac{\partial T}{\partial L_i} = -\frac{\partial}{\partial L_i}\left(\frac{dW_m}{d\theta}\right) \tag{12}$$

The results show that the design parameters having significant influence on the absolute magnitude of magnetic force are L_4, L_5, L_6, and L_{11}. And the tendency of force change can be predicted according to the polarity of sensitivities. For example, if L_4 is increased, within the armature angle between 2° and 3°, the magnetic flux in vertical air gap will increase so that the armature torque or its equivalent force, F also increases. On the contrary, if L_5 is increased, the magnetic flux in horizontal air gap will increase so that the armature torque decreases.

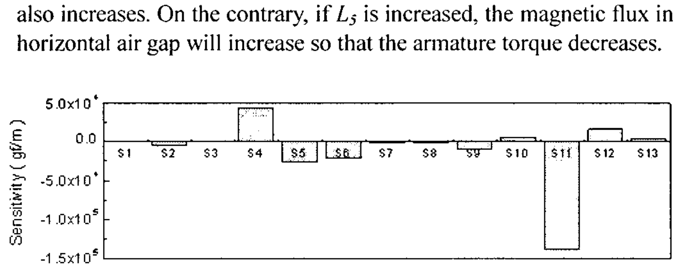

(a) $\theta = 2°$

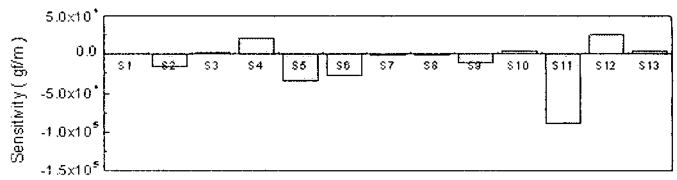

(b) $\theta = 3°$

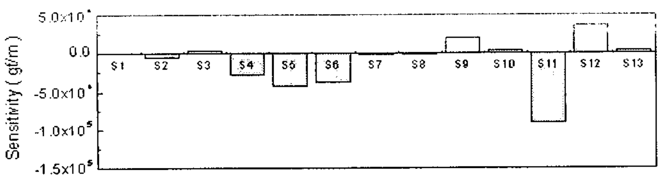

(c) $\theta = 4°$

Fig. 13 Influence of design parameters on force magnitude

As described above, the influence of the design parameters up to 20 items on · the important properties such as force magnitude, gradient of force-to-armature displacement curve could be defined as sensitivity and calculated. By picking out the design parameters with high sensitivity among them, a systematic design process could be constituted, which this study intended to confirm.

5. Conclusions

In this study, a magnetic equivalent circuit for flat-type proportional solenoid was derived, from which the relationship between magnetic force and armature displacement was computed and verified by experimental results.

According to the computed results of magnetic force, there occurred some errors because the magnetic equivalent circuit could not mathematically reflect the local magnetic saturation of iron pole bounded with the reluctances, R_1, R_2, R_3 and R_4 when the armature angle is less than 2°. However, in concern with the armature displacement range where the magnetic force increased and decreased again and with the rate of force change as the armature angle increases, the computed results coincided with the experimental data very closely.

Furthermore, the cause and effect how the design parameters influence the force magnitude and its rate of change with armature rotation was quantitatively expressed by using the magnetic equivalent circuit equation in this study. Therefrom, the length of horizontal air gap and the initial length of vertical air gap turned out to be most important design parameters affecting the force-to-armature displacement curves and this was experimentally proved.

In the future, we are going to derive the rules for analytically determining the range or size of design parameters from given design goals on the basis of the sensitivity analysis. This will expectedly enhance the systemization of the design process which has been usually carried out by the trial and error approach.

REFERENCES

1. Magnet-Schultz, "Products catalog," 2002.
2. Ryu, S. B. and Hong, Y. S., "Design and Experiment of a Miniature 4/3-way Proportional Valve for a Servo-Pneumatic Robot Hand," J. of the Korean Society of Precision Engineering, Vol. 15, No. 12, pp. 142 - 147, 1998.
3. Hong, Y. S., Ha, D. H. and Yeom, M. K., "Design of a Two-dimensional Proportional Solenoid for Miniature Directional Control Pneumatic Valves," KSME Int. J. Vol. 17, No. 7, pp. 978 - 985, 2003.
4. Song, C. S., "Study of an Electro-Hydraulic Proportional Compound Valve," Ph. D. Thesis, KAIST, 1980.
5. Lee, S. H., Jung, K. S. and Baek, Y. S., "Switched Reluctance Contact-Free Linear Actuator Using Attractive Magnetic Forces," J. of the Korean Society of Precision Engineering, Vol. 20, No. 10, pp. 47 - 55, 2003.
6. Lee, S. H. and Baek, Y. S., "Modeling and Analysis of Electromagnets for Magnetic Suspension System," J. of the Korean Society of Precision Engineering, Vol. 20, No. 5, pp. 180 - 188, 2003.
7. Choi, D. J., Rim, C. T. and Kim, S. H., "Modeling of an Inductive Position Sensing System based on a Magnetic Circuit and its Analysis," J. of the Korean Society of Precision Engineering, Vol. 18, No. 6, pp. 93 - 101, 2001.
8. Roters, H. E., "Electromagnetic Devices," New York, John Wiley & Sons Inc., 1964.